Supplenmentary Information

Reconfigurable Parity-Time Symmetry Transition in Phase Change Metamaterials

Tun Cao[a], Ying Cao[a], and Linhan Fang[a]

[a]School of Optoelectronic Engineering and Instrumentation Science, Dalian University of Technology, Dalian 116024, China

E-mail address: caotun1806@dlut.edu.cn

Section 1. The transmission of the phase change metamaterials at different crystallisation ratios.

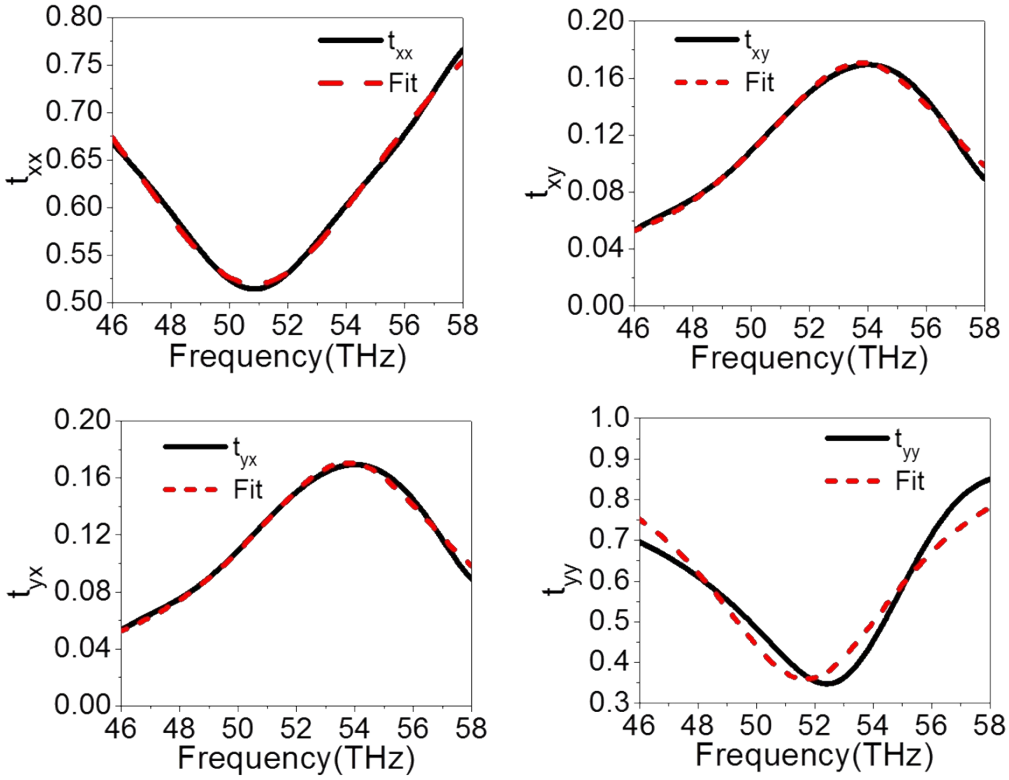

Fig.S1. Simulated (solid lines) and fitted (dashed lines) transmission spectra of the MMs at crystallisation ratio of $q = 0$. The fitted parameters are ξ_x^d, ξ_y^d and C_{xy}.

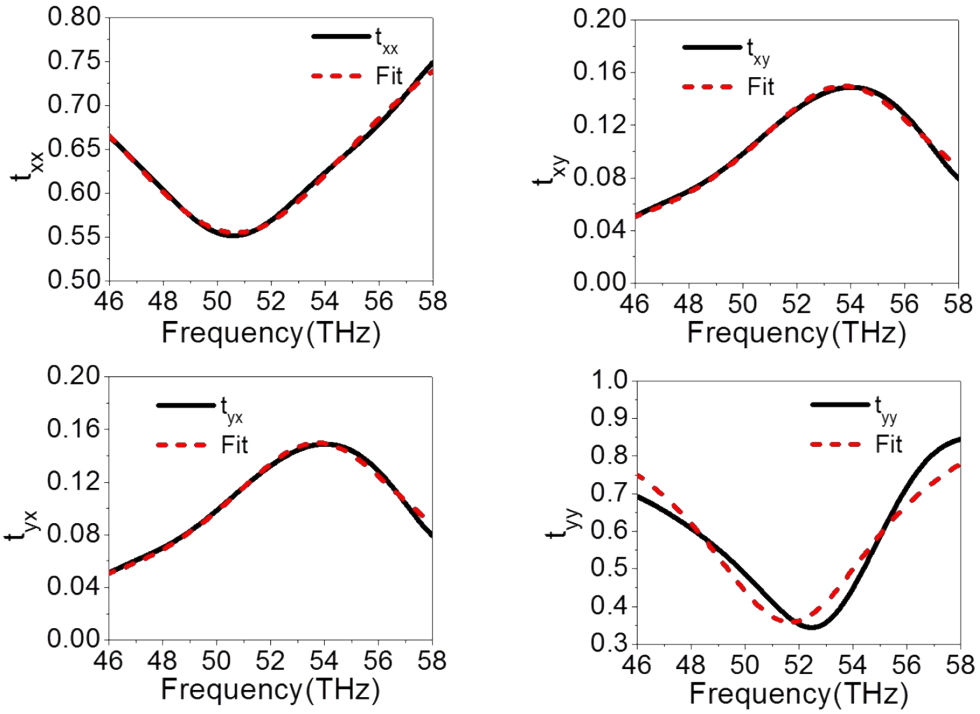

Fig.S2. Simulated (solid lines) and fitted (dashed lines) transmission spectra of the MMs at crystallisation ratio of q = 0.2. The fitted parameters are ξ_x^d, ξ_y^d and C_{xy}.

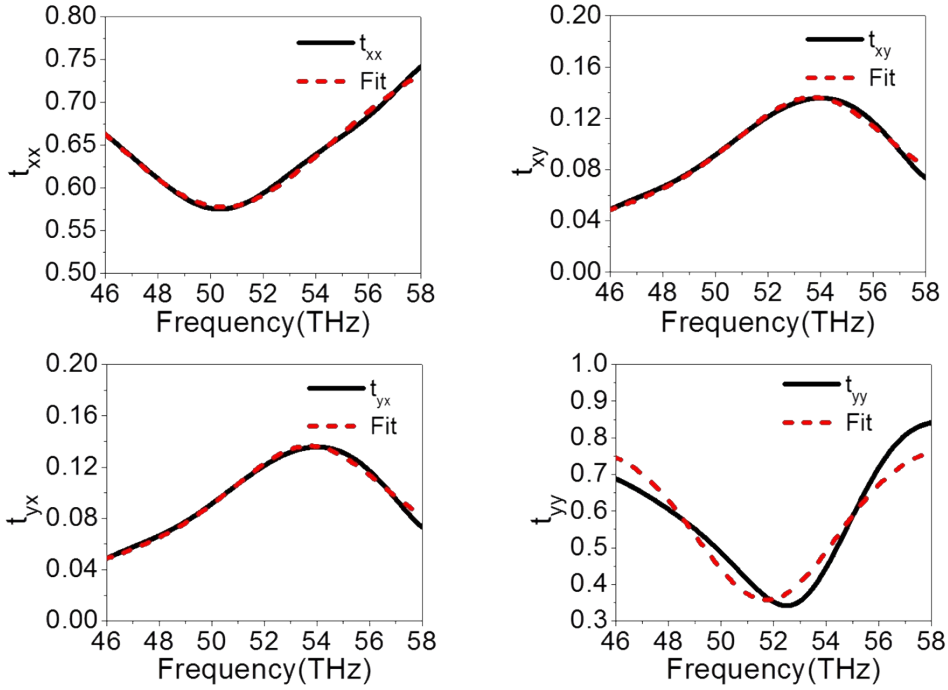

Fig.S3. Simulated (solid lines) and fitted (dashed lines) transmission spectra of the MMs at crystallisation ratio of q = 0.4. The fitted parameters are ξ_x^d, ξ_y^d and C_{xy}.

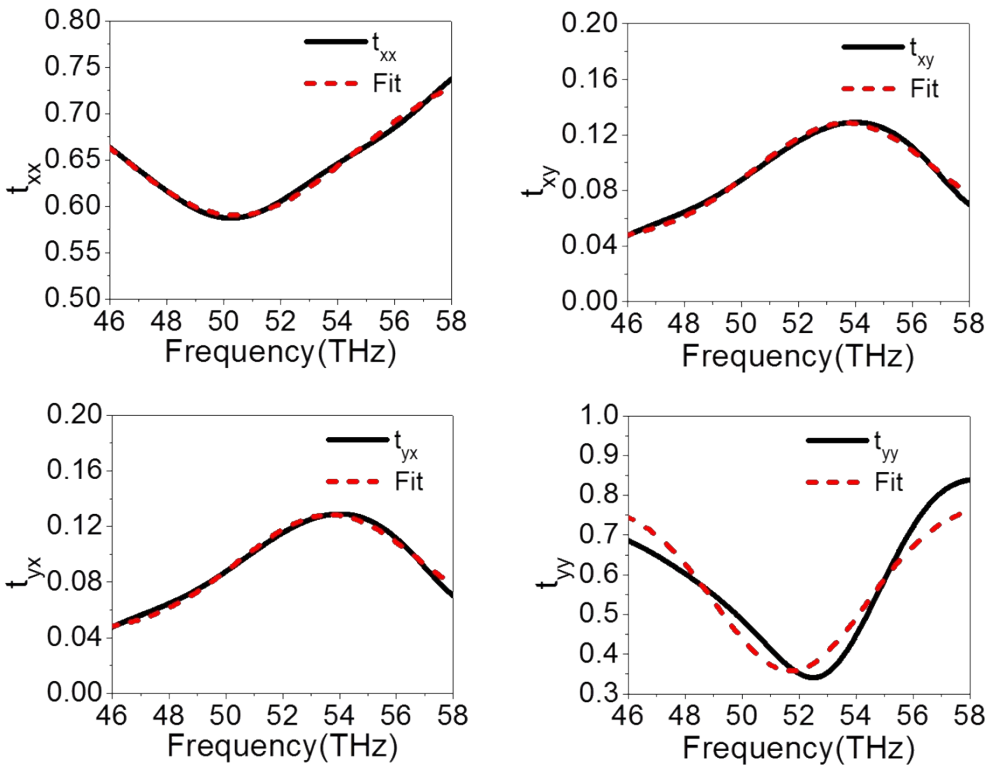

Fig.S4. Simulated (solid lines) and fitted (dashed lines) transmission spectra of the MMs at crystallisation ratio of q = 0.5. The fitted parameters are ξ_x^d, ξ_y^d and C_{xy}.

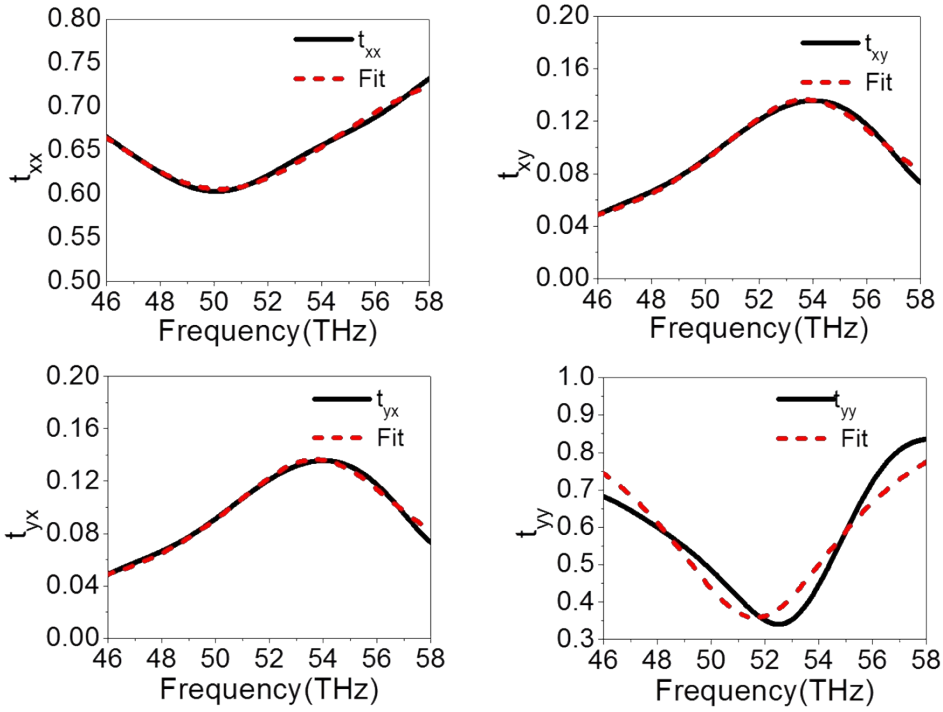

Fig.S5. Simulated (solid lines) and fitted (dashed lines) transmission spectra of the MMs at crystallisation ratio of q = 0.7. The fitted parameters are ξ_x^d, ξ_y^d and C_{xy}.

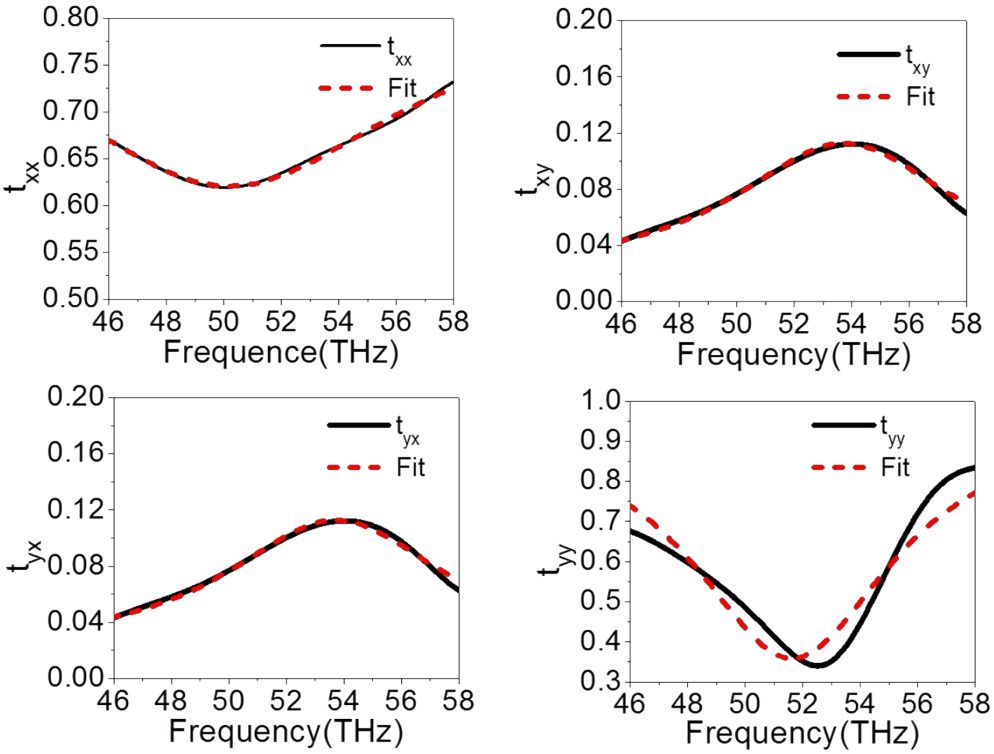

Fig.S6. Simulated (solid lines) and fitted (dashed lines) transmission spectra of the MMs at the crystallisation ratio of q = 1. The fitted parameters are ξ_x^d, ξ_y^d and C_{xy}.

Section 2. The achievement of dissipation loss rate $\xi_{x,y}^d$ and coupling strength C_{xy}.

The complex transmission spectrum is numerically simulated to characterise the phase change metamaterials using CST MICROWAVE STUDIO, where the four possible linear input/output polarisation combinations are obtained to link the incident *E*-field and output *E*-field using the complex Jones matrix[5],

$$\begin{pmatrix} \tilde{E}_x^o(f) \\ \tilde{E}_y^o(f) \end{pmatrix} = \begin{pmatrix} t_{xx}(f) & t_{xy}(f) \\ t_{yx}(f) & t_{yy}(f) \end{pmatrix} \begin{pmatrix} \tilde{E}_x^i(f) \\ \tilde{E}_y^i(f) \end{pmatrix} \tag{S1}$$

Jones matrices calculated in the *xy* basis can be used to predict the transmission of any arbitrarily polarised incident beam through the metamaterial as well as to calculate Jones matrices in any arbitrary basis. A Lorentzian function

$$t(\omega) = A + \frac{g}{\omega - \omega_0 + i\gamma} \tag{S2}$$

is used to fit the calculated eigen transmission spectrum with the various

crystallisation ratios, q shown in Figs.S1-S6 from the supplementary information. Note that, to quantify and ascertain the origin of exceptional point, it is necessary to retrieve the resonant properties of the *x*- and *y*- orientated split ring resonators (SRRs), the dissipation loss rate of each SRR ($\xi_{x,y}^{d}$) and the coupling strength (C_{xy}) between the two SRRs, for the different q. We do this by fitting the Cartesian elements of the transmission matrix using the following Eqs. (s3-s5) derived from Eq.(s2) [5],

$$|t_{xx}(\omega)| = \left| A + \frac{g_x(\omega - \omega_y + i\xi_y^d)}{(\omega - \omega_x + i\xi_x^d)(\omega - \omega_y + i\xi_y^d) - C_{xy}^2} \right| \tag{s3}$$

$$|t_{yy}(\omega)| = \left| A + \frac{g_y(\omega - \omega_x + i\xi_x^d)}{(\omega - \omega_x + i\xi_x^d)(\omega - \omega_y + i\xi_y^d) - C_{xy}^2} \right| \tag{s4}$$

$$t_{xy}(\omega) = \frac{\sqrt{g_x g_y} C_{xy}}{(\omega - \omega_x + i\xi_x^d)(\omega - \omega_y + i\xi_y^d) - C_{xy}^2} \tag{s5}$$

where $\omega_{x,y}$, $\xi_{x,y}^{d}$ and $g_{x,y}$ are the resonant frequencies, dissipation coefficients and oscillator strengths respectively of the *x*- and *y*- orientated SRR, and C_{xy} is the coupling strength. As was seen in Eqs.(s3-s5), the $\xi_{x,y}^{d}$ and C_{xy} are frequency independent.

Section 3. The resonant frequency of the phase change metamaterials at different crystallisation ratios.

In order to obtain a significant variation in ξ_x^d we study the resonant modes around the frequency of f = 51 THz, in which the imaginary part of permittivity (ε_i) of GeTe undergoes a sharp change while the real part of permittivity (ε_r) is equal as switching its state between amorphous and crystalline (see Fig. 1(b)). In Figure S7, we demonstrate the simulated transmission spectra for a set of Ag/GeTe dual-layered SRRs and Cu single-layered SRRs on Si substrate, where the Ag/GeTe dual-layered SRR has the various crystallisation ratios (q) of GeTe ranging from 0 to 1. It is clear to see that the linewidth of the resonant mode changes with q, that in turn, varies the ξ_x^d due to the radical change in ε_i, whilst maintaining a very similar mode frequency

of ~51 THz since the ε_r is equal. By fixing the transmission spectra of the *x*-orientated Ag/GeTe dual-layered SRR using Lorentzian function, we can obtain the resonant frequency as labeled in Figure S7.

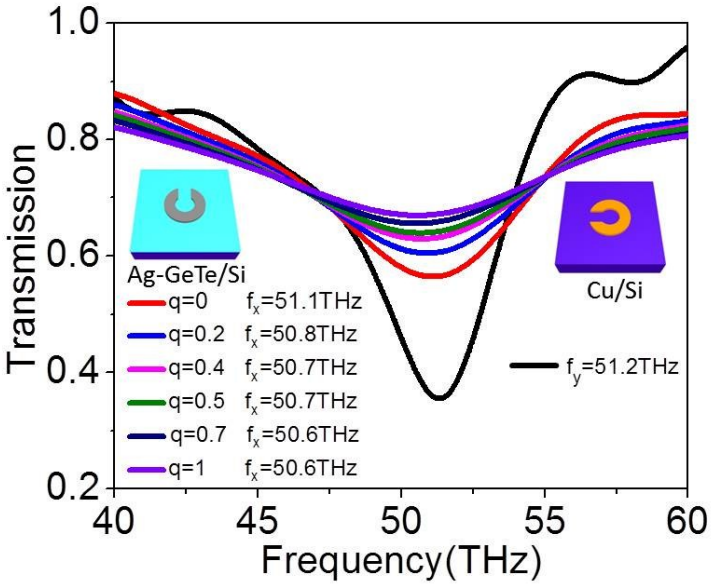

Fig.S7. Simulation of the transmission spectra of the *x*-orientated Ag/GeTe dual-layered SRRs array with the various crytallisation ratios of GeTe (*q*) and *y*-orientated Cu single-layered SRRs array. All the SRRs arrays sit on the Si substrate. The $f_{x,y} = \omega_{x,y} / 2\pi$ are the resonant frequencies of the *x*- and *y*- orientated SRR. The larger *q* leads to a broadening of the linewidth.

Section 4. Thermoelectric model of the phase change metamaterials.

To understand thermoelectric transport in the phase change metamaterials we built a model that includes Joule heating, electrostatics, current crowding and thermoelectric effects[s6]. The electrostatics formula can be written as[s7]

$$\mathbf{J} = \sigma E + \frac{\partial D}{\partial t} + \mathbf{J}_e \qquad \text{(s6)}$$

where $E = -\nabla V_g$ is electric field, $D = \varepsilon_0 \varepsilon_r E$ is electric displacement field norm, $\mathbf{J}$ is electric current density, σ is electric conductivity $\mathbf{J}_e = -\sigma S \nabla T$ is external electric current density, T is temperature, and S is Seebeck coefficient. We can obtain the current density $\mathbf{J}$ under the voltage V_g using Eq.(s6). The Joule heat is achieved by

using $Q = \mathbf{J} \cdot E = -\mathbf{J} \cdot \nabla V_g$, where $Q\,(W/m^3)$ is a volumetric density of heat. By taking Q as a heat source, the heat transfer can be expressed as[s7]

$$\rho C_p \frac{\partial T}{\partial t} + \rho C_p \mathbf{u} \cdot \nabla T = \nabla \cdot (k \nabla T) + Q \qquad \text{(s7)}$$

where ρ is the density of a material, C_p the heat capacity at constant pressure, $\mathbf{u}$ the velocity field, k the thermal conductivity, T the temperature, and $\mathbf{J}_e = -\sigma S \nabla T$. We can thus obtain the time-dependent temperature curve by applying V_g (Fig.5(a)). We built an electric-thermal transfer model to study the temporal change in the temperature of the GeTe within the metamaterials using COMSOL Multiphysics. We employed *Heat Transfer in Solids(ht)* and *Electric Currents(ec)* physics to simulate the electrostatics field and heat transfer, where V_g is the square wave signal that can control the velocity of temperature rising and heating time.

Table S1

	Special heat capacity CS (J / (Kg ·K))	Density ρ(kg/m^3)	Thermal conductivity k(W/(m· k))	Electrical conductivity sigma(S/m)	Relative permittivity epsilnr(1)	Seebeck coefficient S(V/K)
Ag	235[s1]	10500[s1]	429[s1]	Temperature Dependence[s2]	Frequency Dependence[s3]	Temperature Dependence[s2]
Cu	384[s1]	8960[s1]	401[s1]	Temperature Dependence[s2]	Frequency Dependence[s3]	Temperature Dependence[s2]
GeTe	140[s4]	6140[s4]	Temperature Dependence[s4]	Temperature Dependence[s4]	Frequency Dependence[s5]	Temperature Dependence[s4]

Section 5. A comparison between PT-symmetry and non-PT symmetry based metamaterials.

In our proposed PT-symmetry based metamaterials, the eigenstates of the system dominate its polarisation response to an arbitrarily polarised incident light and are therefore important for exploring and engineering the light transmission through the anisotropic photonic medium. This is validated by the strong asymmetric transmission of circularly polarized wave in Fig. S8(a) around the exceptional point (q=0.5). From Fig. 4(e) it was seen that around the exceptional point (EP) the corotating polarisation eigenstates of the phase change metamaterial are nearly circular. This leads to a

significantly asymmetric response to circularly polarised wave with a flat feature for t_{rl} (Fig. S8(a)).

The conventional metamaterials are asymmetric for parity operator or time reversal operator. In our structure, when the two mirror symmetric SRRs have a different resonant frequency or the same dissipation loss rate, the system is non-PT symmetry. In Fig. S8(b), we simulated the non-PT symmetry based metamaterials composed of a pair of identical Cu single-layered SRRs with a mirror symmetry (see inset), where the dissipation loss rate of each SRR is the same ($\xi_y^d = \xi_x^d$).The transmission matrix of the non-PT symmetry metamaterials can thus be expressed as $T = \begin{pmatrix} i(\xi_y^d - \xi_x^d)/2 & -C_{xy} \\ -C_{xy} & i(\xi_x^d - \xi_y^d)/2 \end{pmatrix} = \begin{pmatrix} 0 & -C_{xy} \\ -C_{xy} & 0 \end{pmatrix}$, where $\Delta = \frac{1}{2}\sqrt{4C_{xy}^2 - (\xi_x^d - \xi_y^d)^2} = \pm C_{xy}$ is real and the eigenstate of polarization is fixed. Therefore, the chiroptical response can not be observed; namely, t_{rl} and t_{lr} overlap (see Fig. S8(b)). Recently, studies into metamaterials with varying eigenpolarization states have revealed outstanding wave shaping functionalities such as tunable lenses[63], anomalous reflection and refraction[64], and holography[65], which may benefit from the discovery of reconfigurable Parity-Time Symmetry Transition in phase change metamaterials.

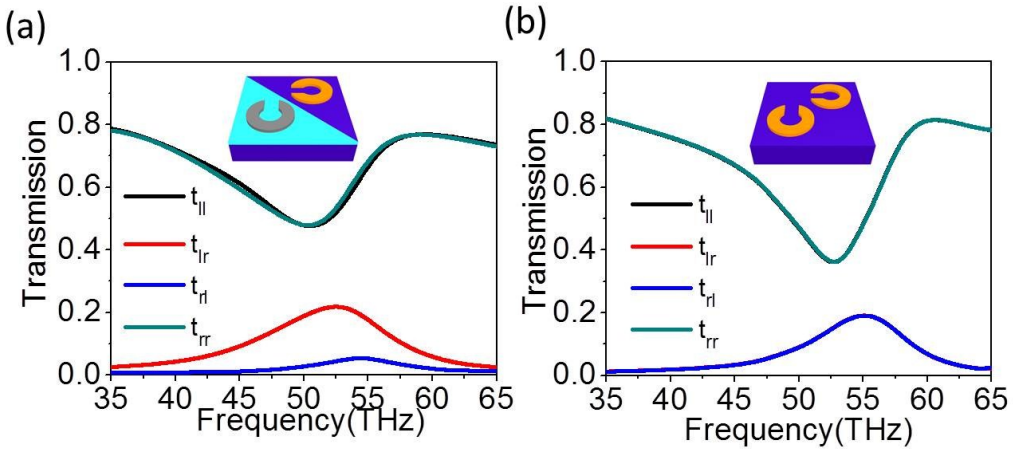

Fig.S8. Circular transmission spectra for (a) the PT-symmetry metamaterials around the EP (q= 0.5), and (b) the conventional metamaterials consisting of a pair of identical Cu single-layered SRRs with a mirror symmetry on Si substrate (see inset). The t_{rr} and t_{ll} correspond to right-to-right and left-to-left polarized transmission conversion efficiencies. t_{lr} stands for right-to-left polarized conversion efficiencies and t_{rl} stands for left-to-right polarized conversion efficiencies in transmission[s8].

References

s1. W. Parker, R. Jenkins, C. Butler and G. Abbott, *J Appl Phys*, 1961, **32**, 1679-1684.

s2. R. A. Matula, *J Phys Chem Ref Data*, 1979, **8**, 1147-1298.

s3. S. Babar and J. Weaver, *Appl Optics*, 2015, **54**, 477-481.

s4. Y. Gelbstein, B. Dado, O. Ben-Yehuda, Y. Sadia, Z. Dashevsky and M. P. Dariel, *Chem. Mater*, 2009, **22**, 1054-1058.

s5. K. Shportko, S. Kremers, M. Woda, D. Lencer, J. Robertson and M. Wuttig, *Nat.Mater*, 2008, **7**, 653.

S6. K. L. Grosse, M.-H. Bae, F. Lian, E. Pop and W. P. King, *Nature nanotechnology*, 2011, **6**, 287.

S7. E. E. Antonova and D. C. Looman, Finite elements for thermoelectric device analysis in ANSYS, 2005.

S8. E. Plum, X.-X. Liu, V. Fedotov, Y. Chen, D. Tsai and N. Zheludev, *Physical review letters*, 2009, **102**, 113902.